Gate tunable terahertz cyclotron emission from two-dimensional Dirac fermions

B. Benhamou-Bui, C. Consejo, S. Krishtopenko, M. Szola, K. Maussang, S. Ruffenach, E. Chauveau, S. Benlemqwanssa, C. Bray, X. Baudry, et al.

APL Photonics

RESEARCH ARTICLE | NOVEMBER 07 2023

Gate tunable terahertz cyclotron emission from two-dimensional Dirac fermions

B. Benhamou-Bui ; C. Consejo ; S. S. Krishtopenko ; M. Szola ; K. Maussang ; S. Ruffenach ; E. Chauveau ; S. Benlemqwanssa; C. Bray ; X. Baudry ; P. Ballet ; S. V. Morozov ; V. I. Gavrilenko ; N. N. Mikhailov ; S. A. Dvoretskii ; B. Jouault ; J. Torres ; F. Teppe

APL Photonics 8, 116106 (2023)
https://doi.org/10.1063/5.0168578

Gate tunable terahertz cyclotron emission from two-dimensional Dirac fermions

Cite as: APL Photon. 8, 116106 (2023); doi: 10.1063/5.0168578
Submitted: 19 July 2023 • Accepted: 16 October 2023 •
Published Online: 7 November 2023

B. Benhamou-Bui,[1] C. Consejo,[1] S. S. Krishtopenko,[1] M. Szola,[1] K. Maussang,[2] S. Ruffenach,[1] E. Chauveau,[1] S. Benlemqwanssa,[2] C. Bray,[1] X. Baudry,[3] P. Ballet,[3] S. V. Morozov,[4,5] V. I. Gavrilenko,[4,5] N. N. Mikhailov,[6,7] S. A. Dvoretskii,[6,8] B. Jouault,[1] J. Torres,[2] and F. Teppe[1,a)]

AFFILIATIONS

[1] Laboratoire Charles Coulomb (L2C), UMR 5221 CNRS-Université de Montpellier, F-34095 Montpellier, France
[2] Institut d'Electronique et des Systèmes (IES), UMR 5214 CNRS-Université de Montpellier, F-34000 Montpellier, France
[3] CEA, LETI, MINATEC Campus, DOPT, Grenoble, France
[4] Institute for Physics of Microstructures of Russian Academy of Sciences, Nizhny Novgorod, Russia
[5] Lobachevsky State University of Nizhny Novgorod, Nizhny Novgorod, Russia
[6] A.V. Rzhanov Institute of Semiconductor Physics, Siberian Branch of Russian Academy of Sciences, Novosibirsk, Russia
[7] Novosibirsk State University, Novosibirsk, Russia
[8] Tomsk State University, Tomsk, Russia

[a)] **Author to whom correspondence should be addressed:** frederic.teppe@umontpellier.fr

ABSTRACT

Two-dimensional Dirac fermions in HgTe quantum wells close to the topological phase transition can generate significant cyclotron emission that is magnetic field tunable in the terahertz frequency range. Due to their relativistic-like dynamics, their cyclotron mass is strongly dependent on their electron concentration in the quantum well, providing a second tunability lever and paving the way for a gate-tunable, permanent-magnet Landau laser. In this work, we demonstrate the proof-of-concept of such a back-gate tunable THz cyclotron emitter at a fixed magnetic field. The emission frequency detected at 1.5 T is centered at 2.2 THz and can already be electrically tuned over 250 GHz. With an optimized gate and a realistic permanent magnet of 1.0 T, we estimate that the cyclotron emission could be continuously and rapidly tunable by the gate bias between 1 and 3 THz, that is to say on the less covered part of the THz gap.

I. INTRODUCTION

The ability to generate and manipulate TeraHertz (THz) waves opens up new avenues for exploring fundamental phenomena and developing innovative technologies in various fields, such as wireless communication, imaging, spectroscopy, and sensing. Several techniques have already been developed, including Schottky diodes,[1] Gunn diodes,[2] resonant tunneling diodes,[3] impact ionizing avalanche transit time diodes,[4] and quantum cascade lasers.[5,6] Nonetheless, none of them are fully tunable over the entire THz gap,[7] and therefore, a compact highly tunable source is still in great demand. In this context, the study of cyclotron emission has emerged as a promising area of research.

The idea of amplification and generation of electromagnetic waves at the frequency of cyclotron resonance (CR) arose in the late 1950s. At that time, the amplification of electromagnetic waves in the CR regime was obtained in plasma[8] and in vacuum electronics.[9,10] Meanwhile, by that time, the cyclotron resonance had already become the standard method for studying the effective masses and band structures of semiconductors[11,12] that naturally yielded the discussion of theoretical possibility of stimulated cyclotron emission in semiconductors. Moreover, the small effective mass in bulk semiconductors gave hope to advance the radiation frequency deep into the THz range. Already, early theoretical studies[13,14] have shown that the non-linear dynamics of the charge carriers in the CR regime is the key ingredient for amplification and generation of

electromagnetic radiation in semiconductors. In particular, Lax[14] was the first who demonstrated that the needed conditions can be achieved in semiconductors with non-parabolic band dispersion, resulting in non-equidistant Landau levels (LLs). The non-equidistance leads to the discrimination of optical transitions up and down from the filled LL, resulting in the possibility of amplification and generation in the CR regime.

Although the ideas of vacuum and semiconductor LL lasers appeared simultaneously, their further development went in completely different ways. The active research of vacuum LL lasers yielded creating of gyrotrons,[15,16] which still remain the most powerful sources of millimeter radiation at present, while investigations of the possibility of semiconductor LL laser realization were actually stopped in the early 1960s. The interest in semiconductor LL lasers resurfaced in the 1970s after the development of the methods for the numerical simulation of the scattering processes in electric and magnetic fields[17,18] which revealed a number of new possibilities for an inverted distribution of the charge carrier, resulting in the realization of light-hole LL lasers[19–24] and CR-based NEMAG (Negative Effective Mass Amplifier and Generator[25]) in bulk p-Ge.[26,27] These two reported p-Ge lasers remain the only semiconductor LL lasers implemented so far. Given the hole mass in germanium, shifting the operation frequencies into the THz range unfortunately requires a substantial magnetic field. This problem, added to the need for an electric field close to the breakdown voltage of the semiconductor, has disqualified this technology in favor of quantum cascade lasers, which are yet poorly tunable in the THz range.

The dual need for a non-parabolic band structure and a very low electronic mass then naturally directs the cyclotron emission research toward graphene and its relativistic massless Dirac fermions.[27–32] However, it turns out to be still possible to find allowed optical transitions reactivating the Auger mechanism and no cyclotron emission has yet been observed there. Alternatively, there are materials that harbor relativistic-like particles other than Dirac fermions with the energy dispersion that can decrease or eliminate Auger recombination inherent in graphene. In particular, as was demonstrated in 2019, HgCdTe bulk films, which host relativistic-like Kane fermions[33–38] in the vicinity of topological phase transition, effectively overcome non-radiative Auger recombinations, enabling the observation of significant Landau emission.[39]

Recently, Landau emission has been reported in HgTe quantum wells (QWs) in the vicinity of topological phase transition.[40] Given that their band structure mimics the one of 2D Dirac fermions,[41–43] the emission proves to be tunable not only by the magnetic field but also by the density of carriers in the QW as measured across eight different samples with varying carrier concentrations. The observation of cyclotron emission from HgTe QWs was direct experimental evidence that additional quadratic terms in the dispersion of Dirac fermions suppresses Auger recombination between Landau levels. Although these experimental findings, indeed, revive the interest to the Dirac materials in the context of tunable LL lasers, the tunability of Landau emission through the variation in the carrier concentration in a single back-gated device has not yet been experimentally demonstrated. The aim of this work is, therefore, to experimentally verify a concept for voltage-tunable THz cyclotron emission from Dirac fermions in HgTe QWs. This, indeed, represents a significant milestone toward the development of a gate-tunable THz Landau laser at a fixed magnetic field operating with a permanent magnet.

II. MATERIAL AND MODEL

The measurements were performed on a HgTe based QW grown by molecular beam epitaxy (MBE) on — (013)-oriented GaAs substrate, followed by a CdTe/ZnTe buffer to relax the lattice mismatch induced strain on the well[44] [see Fig. 1(a)].

To interpret the experimental results, we performed band structure and Landau levels calculations based on the eight-band k· p Hamiltonian for (013)-oriented heterostructures,[45] which directly take into account the interactions between Γ_6, Γ_7, and Γ_8 bands of bulk materials. In the calculations, we also take into account a tensile strain in the layers arising due to the mismatch of lattice constants in the CdTe buffer, HgTe QW, and $Cd_xHg_{1-x}Te$ barriers. The calculations were performed by expanding the envelope wave functions in the basis set of plane waves and by the numerical solution of the eigenvalue problem. The energies of Landau levels (LLs) were found within the so-called axial approximation,[45] while for the calculations of dispersion curves, non-axial terms were held. Details of calculations and the form of the Hamiltonian can be found elsewhere.[45]

Figure 1(b) shows a plot of the LLs' fan chart resulting from this procedure. The non-parabolicity in the energy dispersion is linked to the non-equidistant spacing of LLs, which is a crucial requirement for the observation of cyclotron emission. As discussed in Ref. 40 and observed in Ref. 46, given the values of the classical and quantum mobilities of our material, the system is in the so-called incipient regime, meaning in between a fully continuum of energy and a fully quantized regime [see Fig. 1(b)]. In this regime, several LLs are involved in the cyclotron emission process, and even if Shubnikov–de Haas' oscillations are already well defined, the emission can be treated with the quasi-classical cyclotron resonance formula, where the photon energy is proportional to the magnetic field intensity,

$$E = \frac{\hbar e B}{m_c}, \tag{1}$$

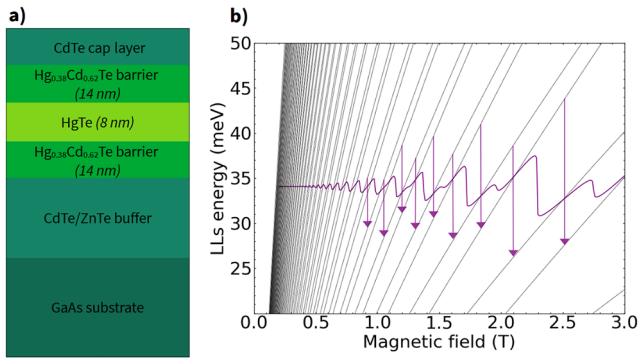

FIG. 1. (a) Sketch of the sample's epitaxial growth. (b) LLs' fan chart computed with the Kane model (solid black lines). The evolution of the Fermi energy, for an electron density of 3.35×10^{11} cm^{-2}, is also plotted (solid purple line). The arrows schematically represent the different inter-level transitions, which contribute to the cyclotron emission.

where e is the electron charge, B is the magnetic field value, $\hbar$ is the Planck constant, and m_c is the cyclotron mass at the Fermi level.

On the basis of the conduction band dispersion, by applying the semiclassical quantization rule, one can predict the behavior of the cyclotron mass with the electron concentration. This dependence allows us to theoretically evaluate the tuning range of the resonant emission energy at a given magnetic field by varying the electron concentration through the use of an electrical gate.

III. EXPERIMENTAL METHODS

The primary concept of the back-gate[47] is to utilize the substrate as a gate dielectric at low temperatures. To enhance the gate capacitance and optimize its efficiency, it is, therefore, crucial to thin down the substrate. The second step consists in gluing the thinned sample on a sample holder. This was performed with conducting silver paint, allowing a high gate voltage to be applied on the backside of the sample. In this work, voltages ranging from −200 to +200 V were applied, limited by the breaking voltage thresholds of the substrate.[47]

An alternative method of tuning the carrier concentration in the HgTe QW involves utilizing the persistent photoconductivity (PPC) effect, also known as "optical gating." This approach is often more convenient compared to fabricating gate structures.[48] The PPC phenomenon has been observed in various semiconductor materials, typically resulting in enhanced conductivity under illumination.[49] This optical gating led in our case to a notable increase in the carrier concentration in the HgTe QW.

The high energy LLs are populated, thanks to short electrical pulses of frequency 127 Hz and a typical peak-to-peak amplitude of 8 V. The pulses are injected in the sample via indium balls welded at the surface of the sample, enabling us to have ohmic contacts when it diffuses in the whole structure. The typical distance between two contacts is 2–3 mm, giving rise to electric fields in the sample of typically hundredth of V cm^{-1}. We used a unique Landau spectrometer (see the supplementary material for the detailed experimental setup) integrated in a cryostat, along with three superconducting coils. The n-InSb detector placed in the center of one of these magnets requires, indeed, a strong magnetic field to narrow and tune its detection's energy window. The second of the three coils is used to split the conduction and valence bands of our sample into LLs, and the last one allows us to compensate the influence of the other two coils on each other. Each measurement was performed at a constant magnetic field value on the sample while scanning the magnetic field on the detector, thereby scanning the detection energy (E_{det}). The electrical signal on the detector is processed through a low-noise preamplifier and a lock-in amplifier. All the measurements were performed at 4.2 K.

IV. EXPERIMENTAL RESULTS

Figure 3(a) shows an example of the results that we obtained for a gate voltage of $V_g = 0$ V. We can see a waterfall plot of the electrical signal measured on the n-InSb detector, each curve being recorded at a different magnetic field applied on the sample.

Every curve features a peak at a defined energy, witnessing a Landau emission coming out of the QW. It seems that this emission energy is growing with the magnetic field applied. It is confirmed with Fig. 3(b), which depicts a colormap of the complete dataset obtained for this particular gate voltage value. The emission energy evolves linearly with the magnetic field applied on the sample, in accordance with the semi-classical cyclotron formula (1) . From a linear fit, one can extract the value of the cyclotron mass. The associated electron density, induced by the gate effect, is determined through magneto-transport experiments by measuring the frequency of Shubnikov–de Haas' oscillations.[50] By doing such a study for different values of back-gate voltage, one can follow the evolution of the emission peak with the gate bias and deduce the evolution of the cyclotron mass with the latter. The inset of Fig. 3(b) shows the experimental values of cyclotron mass extracted for three extreme gate voltage values: −200, 0, and +200 V. We can see that the experimental points are in good agreement with the prediction of the Kane model (black dashed line), as already observed.[51] Although Landau emission can be generated from both edge and bulk states,[52] we believe that the observed emission comes from the bulk states in our sample. Indeed, (i) we are in a regime of strong electric bias, which considerably disrupts the edge states and favors the current flow through the bulk states,[53] (ii) the system is not yet in the well-established quantum Hall regime but rather in the Shubnikov–de Haas regime, and (iii) given the geometry of our sample, the ratio of active surfaces between the edges and the bulk makes the contribution of the edges negligible.

An extra experimental point is also measured by persistent photoconductivity (PPC) doping with a 660 nm illumination. The carrier density can, indeed, be modulated in HgTe based QWs, thanks to a monochromatic radiation.[54] The expected photoinduced increase in carrier density confirms the decrease in the emission frequency and enhances its tunability range. However, there is a clear increase in the width of the cyclotron resonance when PPC is used. This broadening cannot be solely attributed to the rising number of Landau levels involved in the cyclotron resonance with increasing carrier density. This additional broadening remains

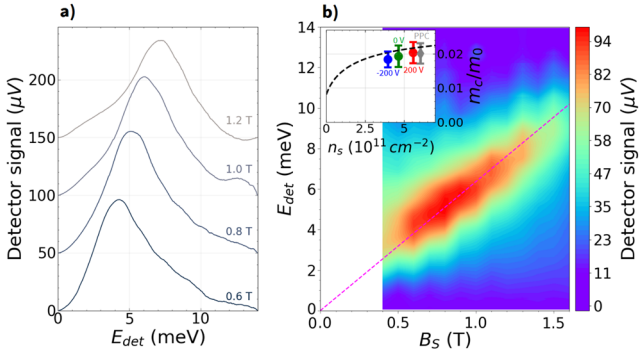

FIG. 2. (a) Waterfall plot of the electrical signal on the n-InSb detector, witnessing an emission of photons, at zero gate voltage and for various magnetic field values. (b) Colormap of the evolution of the emission energy with the magnetic field applied on the sample. The dashed magenta line is a linear fit, based on formula (1), allowing us to extract the cyclotron mass value. Experimental values of cyclotron mass for different electron density values are shown in the inset. The value of the gate bias is indicated along with the experimental point. The predicted behavior, obtained with the Kane model, is plotted as the black dashed line. The PPC point is added in gray.

unexplained, but it may be linked to either the sample's non-uniformity or the photoinduced modification in the QW's potential. Further experimental and theoretical investigation is required to clarify this phenomenon.

As a proof of concept, we performed cyclotron emission measurements at a fixed low magnetic field of 1.5 T for different values of the gate voltage applied. Figure 2(a) shows the evolution of the emission peak's energy when we scan the gate bias from −130 V to +150 V. The change in energy is about 1 meV, which corresponds to ~250 GHz. This is evidenced more clearly in Fig. 2(b), where the peak maxima are extracted and plotted as a function of the gate voltage value. These results show a tunability of the emission frequency with the gate voltage value applied, around 2.2 THz and in a range of almost 200 GHz, which gives an electrical tunability of 485 ± 2 MHz/V. Again, we added a curve obtained by PPC doping [in gray in Fig. 2(a)] to prove that it is possible to increase even more the emission's energy by adding more electrons in the QW.

V. DISCUSSION

In comparison with p-doped germanium, and without considering population inversion and laser action processes, HgTe QWs offer numerous advantages as cyclotron emitters. First, due to the two-dimensional nature of the system, it inherently allows for the use of an electrical carrier density modulation gate, enabling the emission to be tuned at a fixed magnetic field and, thus, allowing the use of a permanent magnet. Second, the cyclotron mass of Dirac fermions in HgTe QWs, even with a small gap, is lower ($0.018 \cdot m_0$ at zero gate bias) than that of holes in p-Ge ($0.047 \cdot m_0$).[22] This enables the generation of cyclotron emission within the THz range at significantly lower magnetic fields compared to those employed with p-Ge (more than 3 T).[22]

One interesting observation from the inset of Fig. 3(b) is that the carrier concentrations we are working with are relatively high. According to the predictions of the Kane model, the corresponding

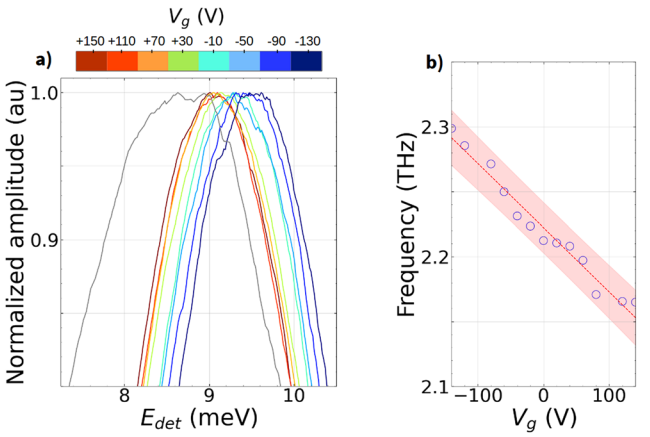

FIG. 3. (a) Normalized emission spectra for various values of gate voltage, obtained at a fixed magnetic field value of 1.5 T. For the sake of clarity, not all spectra are represented. We have added a spectrum obtained with PPC doping in gray. (b) Extracted emission position, converted into frequency, as a function of the applied gate voltage value. The red dashed line is the best linear fit obtained, and the shaded area corresponds to the 95% confidence interval.

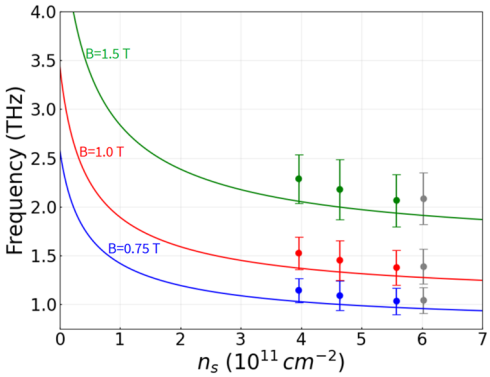

FIG. 4. Predicted evolution of the cyclotron frequency with the electron density for three different values of magnetic field (solid lines). The experimental points were obtained by injecting the experimental cyclotron mass values of the inset of Fig. 3(b) in formula (1) for the corresponding magnetic field values. The gray points are obtained with the red LED on.

slope of the effective mass in this range is rather low. As illustrated in Fig. 4, the frequency variation in relation to the carrier concentration demonstrates a nonlinear pattern that becomes more pronounced at lower doping levels. Consequently, it would be worthwhile to investigate lower electron density values in order to achieve more efficient tuning of the emission frequency with minimal carrier modulation.

Various approaches can be considered to accomplish this goal. One way is to enhance the gate efficiency from the backside through a more sophisticated technological process, possibly involving the use of an alternative dielectric material. In addition, the gate efficiency can also be improved from the top by employing semi-transparent gates, typically used in magneto-transmission experiments.[55,56] Another option is to grow samples with lower doping levels, allowing us to operate directly within the highly non-linear range in which even a small change in the carrier concentration leads to a significant variation in cyclotron mass and, consequently, in cyclotron frequency. It was reported that HgTe quantum wells with low doping can be grown by utilizing the effect of Hg vacancies.[47] If we consider the possibility of growing a QW with a zero gate bias density of around 2×10^{11} cm^{-2} and assume the same level of gate efficiency demonstrated in this study [specifically, $\Delta n = 1.5 \times 10^{11}$ cm^{-2} as shown in the inset of Fig. 3(b)], it would result in a much greater range of tunability in the emission frequency. Indeed, under these conditions, it would be possible to achieve a wide range of electron densities, ranging from 5×10^{10} to 3.5×10^{11} cm^{-2}. If we now report these concentrations in Fig. 4, which shows the Kane model's predictions in terms of emission frequency, we would observe a continuous tunability from 2.1 to 3.5 THz at a magnetic field value of 1.5 T. This would result in a tunability range of 4.5 GHz/V, which is nearly ten times greater than what we have demonstrated in this study.

In Fig. 4, the theoretical tunability of a cyclotron source based on HgTe QWs is depicted for three distinct magnetic field values. The 0.75 and 1 T values, achievable with a permanent magnet, provide realistic/practical insights into the frequency range in which such a compact source could effectively operate. It is worth emphasizing that despite the current limited tunability of the source, the

underlying principle holds great potential. Such an emitter could be finely tuned to operate within the most challenging portion of the THz range. At a magnetic field strength of 1 T, the source's tunability could, indeed, span from 1 to 3 THz by varying the carrier concentration from 1×10^{11} to 3×10^{11} cm^{-2}. To summarize, lower frequencies and tunability in the 1 THz range are achievable with lower magnetic fields, with incremental technical improvements in device fabrication, and with a lower intrinsic doping of quantum wells.

VI. CONCLUSION AND OUTLOOKS

In summary, our study successfully demonstrated the proof of concept for a gate-tunable THz cyclotron source at a fixed magnetic field, by utilizing the Landau emission from 2D Dirac fermions in HgTe QWs through a straightforward technological process involving substrate thinning and a basic back-gate. Such a source holds the potential for modulation speeds reaching the GHz range, surpassing the limitations of magnetic field variation. Improving the device manufacturing process should make it possible to reduce the initial doping level of the device and, consequently, to increase the tunability range of the THz source with much lower gate voltages.[57] These findings pave the way for the development of a Landau laser capable of continuous tuning within the THz range, solely through the modulation of an electrical gate voltage, while maintaining a fixed magnetic field provided by a permanent magnet.

SUPPLEMENTARY MATERIAL

In the supplementary material, we describe in detail the band-structure calculation of the material as well as the experimental setup and the sample processing.

ACKNOWLEDGMENTS

This work was supported by the TeraHertz Occitanie Platform, the CNRS through IRP "TeraMIR" by the French Agence Nationale pour la Recherche (ANR) for Equipex+ Hybat (ANR-21 -ESRE-0026) project, by the European Union and the ANR for Flag-Era JTC 2019 DeMeGRaS project (ANR-19-GRF1-0006-03), and the Center of Excellence (Center of Photonics), funded by the Ministry of Science and Higher Education of the Russian Federation (Contract No. 075-15-2022-316; S.V.M., V.I.G.). We would like to thank Laurent Bonnet and Nassim Mouelhi for technical support.

AUTHOR DECLARATIONS

Conflict of Interest

The authors have no conflicts of interest to declare.

Author Contributions

B. Benhamou-Bui: Data curation (lead); Formal analysis (lead); Investigation (lead); Writing – original draft (lead). **C. Consejo**: Investigation (lead); Methodology (lead); Writing – review & editing (equal). **S. S. Krishtopenko**: Formal analysis (equal); Writing – review & editing (equal). **M. Szola**: Investigation (equal); Writing – review & editing (equal). **K. Maussang**: Writing – review & editing (equal). **S. Ruffenach**: Supervision (equal). **E. Chauveau**: Investigation (equal). **S. Benlemqwanssa**: Investigation (equal). **C. Bray**: Supervision (equal). **X. Baudry**: Investigation (equal). **P. Ballet**: Supervision (equal); Writing – review & editing (equal). **S. V. Morozov**: Supervision (equal); Writing – review & editing (equal). **V. I. Gavrilenko**: Supervision (equal); Writing – review & editing (equal). **N. N. Mikhailov**: Supervision (equal); Writing – review & editing (equal). **S. A. Dvoretskii**: Supervision (equal). **B. Jouault**: Supervision (equal); Writing – review & editing (equal). **J. Torres**: Supervision (equal); Writing – review & editing (equal). **F. Teppe**: Conceptualization (lead); Supervision (equal); Writing – review & editing (equal).

DATA AVAILABILITY

The data that support the findings of this study are available within the article.

REFERENCES

[1] J. Ward *et al.*, "Capability of THz sources based multiplier TH6B-4 on Schottky diode frequency chains," in *IEEE MTT-S Digest* (IEEE, 2004).
[2] H. Eisele and R. Kamoua, "Submillimeter-wave InP Gunn devices," in *IEEE Transactions on Microwave Theory and Techniques* (IEEE, 2004).
[3] M. Asada *et al.*, "Resonant tunneling diodes for sub-terahertz and terahertz oscillators," Jpn. J. Appl. Phys. **47**, 4375–4384 (2008).
[4] M. Mukherjee *et al.*, "GaN IMPATT diode: A photo-sensitive high power terahertz source," Semicond. Sci. Technol. **22**, 1258 (2007).
[5] J. Faist *et al.*, "Quantum cascade laser," Science **264**, 553–556 (1994).
[6] B. S. Williams, "Terahertz quantum-cascade lasers," Nat. Photonics **1**, 517–525 (2007).
[7] C. Sirtori, "Bridge for the terahertz gap," Nature **417**, 132–133 (2002).
[8] R. Q. Twiss, "Radiation transfer and the possibility of negative absorption in radio astronomy," Aust. J. Phys. **11**, 564 (1958).
[9] R. Pantell, "Backward-wave oscillators in an unloaded waveguide," Proc. IRE **47**, 1146 (1959).
[10] J. Schneider, "Stimulated emission of radiation by relativistic electrons in a magnetic field," Phys. Rev. Lett. **2**, 504 (1959).
[11] G. Dresselhaus *et al.*, "Cyclotron resonance of electrons and holes in silicon and germanium crystals," Phys. Rev. **98**, 368 (1955).
[12] R. N. Dexter *et al.*, "Cyclotron resonance experiments in silicon and germanium," Phys. Rev. **104**, 637 (1956).
[13] A. S. Tager *et al.*, "Use of cyclotron resonance in semiconductors for the amplification and generation of microwaves," Sov. Phys. JETP **8**, 560 (1959).
[14] B. Lax, "Cyclotron resonance and impurity levels in semiconductors," in *Quantum Electronics: Proceedings of a Symposium* (Columbia University Press, 1960), p. 428.
[15] V. Flyagin *et al.*, IEEE Trans. Microwave Theory Tech. **25**, 514 (1977).
[16] A. V. Gaponov *et al.*, Int. J. Electron. **51**, 277 (1981).
[17] Y. I. Al'ber *et al.*, "Inverted hot-electron states and negative conductivity in semiconductors," Sov. Phys. JETP **45**, 539 (1977).
[18] V. N. Shastin *et al.*, "Population inversion and hf negative conductivity in degenerate band under optical excitation," Fiz. Tech. Polupr. **14**, 557 (1980).
[19] Ivanov *et al.*, "Stimulated Landau level emission in p-Ge," Sov. Tech. Lett. **9**, 264–268 (1983).
[20] A. A. Andronov *et al.*, "Stimulated emission in the long-wavelength IR region from hot holes in Ge in crossed electric and magnetic field," Sov. Phys.-JETP Lett. **25**, 804 (1984).
[21] S. Komiyama *et al.*, "Evidence for induced far-infrared emission from *p*-Ge in crossed electric and magnetic fields," Appl. Phys. Lett. **47**, 958 (1985).

[22]K. Unterrainer *et al.*, "Tunable cyclotron-resonance laser in germanium," Phys. Rev. Lett. **64**, 2277 (1990).
[23]Y. L. Ivanov *et al.*, "Population inversion in the set of light hole Landau levels in germanium," Semicond. Sci. Technol. **7**, B636 (1992).
[24]O. A. Klimenko *et al.*, "Terahertz wide range tunable cyclotron resonance p-Ge laser," J. Phys.: Conf. Ser. **193**, 012064 (2009).
[25]A. A. Andronov *et al.*, "Population inversion and CR negative differential conductivity of heavy hole in Ge under streaming," Fiz. Tech. Polupr. **16**, 212 (1982).
[26]A. A. Andronov *et al.*, "Germanium hot-hole cyclotron-resonance maser with negative effective hole masses," Sov. Phys. JETP **63**, 211 (1986).
[27]T. Morimoto *et al.*, "Cyclotron radiation and emission in graphene—A possibility of Landau-level laser," J. Phys.: Conf. Ser. **150**, 022059 (2009).
[28]Y. Wang *et al.*, "Continuous-wave lasing between Landau levels in graphene," Phys. Rev. A **91**, 033821 (2015).
[29]F. Wendler and E. Malic, "Towards a tunable graphene-based Landau level laser in the terahertz regime," Sci. Rep. **5**, 12646 (2015).
[30]S. Brem *et al.*, "Microscopic modeling of tunable graphene-based terahertz Landau-level lasers," Phys. Rev. B **96**, 045427 (2017).
[31]F. Wendler *et al.*, "Symmetry-breaking supercollisions in Landau-quantized graphene," Phys. Rev. Lett. **119**, 067405 (2017).
[32]S. Brem *et al.*, "Electrically pumped graphene-based Landau-level laser," Phys. Rev. Mater. **2**, 034002 (2018).
[33]M. Orlita *et al.*, "Observation of three-dimensional massless Kane fermions in a zinc-blende crystal," Nat. Phys. **10**, 233–238 (2014).
[34]F. Teppe *et al.*, "Temperature-driven massless Kane fermions in HgCdTe crystals," Nat. Commun. **7**, 12576 (2016).
[35]S. Krishtopenko and F. Teppe, "Relativistic collapse of Landau levels of Kane fermions in crossed electric and magnetic fields," Phys. Rev. B **105**, 125203 (2022).
[36]K.-M. Dantscher *et al.*, "Photogalvanic probing of helical edge channels in two-dimensional HgTe topological insulators," Phys. Rev. B **95**, 201103 (2017).
[37]S. Morozov *et al.*, "Coherent emission in the vicinity of 10 THz due to Auger-suppressed recombination of Dirac fermions in HgCdTe quantum wells," ACS Photonics **8**, 3526–3535 (2021).
[38]V. Aleshkin *et al.*, "Radiative recombination in narrow gap HgTe/CdHgTe quantum well heterostructures for laser applications," J. Phys.: Condens. Matter **30**, 495301 (2018).
[39]D. But *et al.*, "Suppressed Auger scattering and tunable light emission of Landau-quantized massless Kane electrons," Nat. Photonics **13**, 783–787 (2019).
[40]S. Gebert *et al.*, "Terahertz cyclotron emission from two-dimensional Dirac fermions," Nat. Photonics **17**, 244–249 (2023).
[41]B. Büttner *et al.*, "Single valley Dirac fermions in zero-gap HgTe quantum wells," Nat. Phys. **7**, 418–422 (2011).
[42]M. Marcinkiewicz *et al.*, "Temperature-driven single-valley Dirac fermions in HgTe quantum wells," Phys. Rev. B **96**, 035405 (2017).
[43]A. M. Kadykov *et al.*, "Temperature-induced topological phase transition in HgTe quantum wells," Phys. Rev. Lett. **120**, 086401 (2018).
[44]S. Dvoretsky *et al.*, "Growth of HgTe quantum wells for IR to THz detectors," J. Electron. Mater. **39**, 918–923 (2010).
[45]S. Krishtopenko *et al.*, "Pressure- and temperature-driven phase transitions in HgTe quantum wells," Phys. Rev. B **94**, 245402 (2016).
[46]M. Orlita *et al.*, "Classical to quantum crossover of the cyclotron resonance in graphene: A study of the strength of intraband absorption," New J. Phys. **14**, 095008 (2012).
[47]M. Baenninger *et al.*, "Fabrication of samples for scanning probe experiments on quantum spin hall effect in HgTe quantum wells," J. Appl. Phys. **112**, 103713 (2012).
[48]I. Nikolaev *et al.*, "Bipolar persistent photoconductivity in HgTe/CdHgTe double quantum well heterostructures and its application for reversible change in the conductivity type," J. Appl. Phys. **132**, 234301 (2022).
[49]K. E. Spirin *et al.*, "Bipolar persistent photoconductivity in HgTe/CdHgTe (013) double quantum-well heterostructures," Semiconductors **52**, 1586–1589 (2018).
[50]N. W. Ashcroft and N. D. Mermin, *Solid State Physics* (EDP Science, 2002).
[51]A. V. Ikonnikov *et al.*, "Cyclotron resonance and interband optical transitions in HgTe/CdTe(013) quantum well heterostructures," Semicond. Sci. Technol. **26**, 125011 (2011).
[52]K. Ikushima and S. Komiyama, "Photon generation by injection of electrons via quantum hall edge channels," Phys. Rev. B **84**, 155313 (2011).
[53]K. Panos *et al.*, "Current distribution and Hall potential landscape towards breakdown of the quantum Hall effect: A scanning force microscopy investigation," New J. Phys. **16**, 113071 (2014).
[54]K. E. Spirin *et al.*, "Residual-photoconductivity spectra in HgTe/CdHgTe quantum-well heterostructures," Semiconductors **53**, 1363–1366 (2019).
[55]J. Lloyd-Hughes, "Terahertz spectroscopy of quantum 2D electron systems," J. Phys. D: Appl. Phys. **47**, 374006 (2014).
[56]K. Muro *et al.*, "Far-infrared cyclotron resonance of two-dimensional electrons in an $Al_xGa_{1-x}As/GaAs$ heterojunction," Surf. Sci. **113**, 321–325 (1982).
[57]E. Ma *et al.*, "Unexpected edge conduction in mercury telluride quantum wells under broken time-reversal symmetry," Nat. Commun. **6**, 7252 (2015).